

Effects of Mg Concentration of $Mg_xZn_{1-x}O$ Nanostructure Thin Films by PLD on Optical and Topographical Properties

Dr. Adawiya J. Haidar 

Nanotechnology and advanced materials research center, University of Technology/Baghdad
Email: adawiya_haider@yahoo.com

Dr. Jehan A. Saimon

Applied Science Department, University of Technology/Baghdad

Ali J. Addie

Directorate of Chemistry & Physics of Mat. Res. /Ministry of Science & Technology/Baghdad

Revised on: 30/10/2012 & Accepted on: 9/5/2013

ABSTRACT

In this work, $Mg_xZn_{1-x}O$ thin films were synthesized by pulsed laser deposition technique, the morphology and optical properties of $Mg_xZn_{1-x}O$ films were characterized by Atomic force microscopy (AFM) and UV-VIS spectroscopy. The $Mg_xZn_{1-x}O$ films have been deposited on sapphire substrates with different Mg contents ($x=0, 0.1, 0.2, 0.3, 0.4, 0.6, 0.8, 1$), using double frequency Q-switching Nd:YAG laser (532nm), repetition rate (6 Hz) and a pulse duration of (7 ns).

The present of hexagonal and cubic structure of $Mg_xZn_{1-x}O$ thin films was shown from X-ray diffraction measurement. The optical transmission results show that the transparency of the $Mg_xZn_{1-x}O$ films are greater than 85% in the visible region which increases with the increasing of Mg content. The absorption can be extended to lower wavelength range with higher magnesium contents, which can improve the transparency in the ultraviolet wavelength range. The band gap energy was found to be changed to the higher energy side with the increasing of Mg concentration. By changing Mg content from $x=0$ to $x=1$, the optical band gap of $Mg_xZn_{1-x}O$ films can be tuned from 3.4 eV to 5.9 eV, while the refractive index decreases from (1.96 – 1.75) as Mg-content increases from (0 to 1) at constant wavelength 400nm. This provides an excellent opportunity for bandgap engineering for optoelectronic applications. It is found from the AFM studies that the surface roughness of the films decreases with increasing the Mg content and the smallest grain size (33.8nm) with Mg content (1).

Keywords: Pulsed Laser Deposition (PLD), $Mg_xZn_{1-x}O$ Thin Films, Nonstructural, Optoelectronic Applications.

دراسة تأثير محتوى المغنسيوم في اغشية $Mg_xZn_{1-x}O$ على الخصائص البصرية والطوبوغرافية

الخلاصة

الهدف من البحث هو تحضير اغشية رقيقة من اوكسيد الخارصين - مغنسيوم ($Mg_xZn_{1-x}O$) باستخدام تقنية الترسيب بالليزر النبضي ودراسة الخصائص التركيبية باستخدام مجهر القوى الذرية، بالإضافة الى دراسة الخصائص البصرية لتلك الاغشية (طيف النفاذية المرئي وفوق البنفسجي). جرى دراسة نمو الاغشية عند درجة حرارة $300^\circ C$ على قواعد الالومينا وكثافة طاقة الليزر الساقطة $1.6 J/cm^2$ وباختلاف محتوى المغنسيوم ($x= 0, 0.1, 0.2, 0.3, 0.4, 0.6, 0.8, 1$) باستعمال ليزر النيديميوم-ياك الذي يعمل بتقنية عامل النوعية عند الطول الموجي $532nm$ بمعدل تكرارية (6Hz). وضحت قياسات حيود الاشعة السينية وجود التركيب السداسي والمكعب لاغشية $Mg_xZn_{1-x}O$. كانت نتائج النفاذية البصرية اعلى من 85% لاغشية اوكسيد الخارصين مغنسيوم بالمنطقة المرئية من الطيف وتزداد بازدياد محتوى المغنسيوم. كما يمتد الامتصاص باتجاه الاطوال الموجية الاقصر عند محتوى المغنسيوم الاعلى مما يحسن من مقدار النفاذية عند الاطوال الموجية فوق البنفسجية. وجد تغير فجوة الطاقة لاغشية اوكسيد الخارصين مغنسيوم المرسبة على قواعد الالومينا باتجاه الطاقات الاعلى بزيادة تركيز المغنسيوم. اذ تتغير فجوة الطاقة البصرية من 3.4 الى 5.9 الكترون فولت عند تغيير محتوى المغنسيوم من 0 الى 1 , بينما يقل معامل الانكسار من 1.75- 1.96 عند ثبوت الطول الموجي (400) نانومتر، كما لوحظ تأثير مثبت للمغنسيوم على نمو الحبيبات في الاغشية المحضرة.

INTRODUCTION

One interesting feature of zinc oxide (ZnO) is that can be alloyed with magnesium oxide in order to form $Mg_xZn_{1-x}O$ semiconductor alloys [1]. The alloys have tunable band gap which raises the possibility of band gap engineered heterostructures with less lattice mismatched alternative layers such as $MgZnO/ZnO/MgZnO$ and $MgZnO/CdZnO/MgZnO$.

Band gap engineering of ZnO is essential to realize low dimensional structures such as Quantum wells and super-lattices [2]. In order to make progress in modern devices, like ZnO UV detector and field effect transistors (FET), modulation of the band gap is required. By alloying the starting semiconductor with another material of different band gap, the band gap of the resultant alloy material can be fine tuned, thus affecting the wavelength of exciton emissions [3].

It has been verified due to the development of $Mg_xZn_{1-x}O$ and $Be_zZn_{1-z}O$ alloys for larger band gap material and $Cd_yZn_{1-y}O$ alloy for smaller band gap material, allowing band gap tuning in a wide range [1,4,5].

The energy gap $E_g(x)$ of a ternary semiconductor AZn_xO_{1-x} (where $A=Mg, Be$ or Cd) is determined by the following empirical equation [6]:

$$E_g(x) = (1-x)E_{ZnO} + xE_{AO} - bx(1-x) \quad \dots (1)$$

Where b is the bowing parameter and E_{AO} and E_{ZnO} are the band gap energies of compounds AO (MgO, CdO, BeO) and ZnO , respectively. The bowing parameter depends on the difference in the electronegativities of the end binaries ZnO and AO .

Among the doped or alloyed ZnO compounds, the most interesting case seems to be $Mg_xZn_{1-x}O$ according to the very specific structural and physical properties [7-9], which can be obtained as a function of the Mg concentration: By changing the Mg concentration from $x=0$ to $x=1$, the band gap of this compound can be tuned from 3.3 to 7.8 eV.

In this paper, the effect of different Mg concentrations on the structure, optical and morphology of $Mg_xZn_{1-x}O$ thin films was studied.

EXPERIMENTS DETAILS

$Mg_xZn_{1-x}O$ thin films were synthesized by pulsed laser deposition technique. The focused Nd:YAG SHG Q-switching laser beam at 532nm (pulse width 7nsec, repetition frequency 6 Hz) for 40 laser pulse is incident on the target surface making an angle of 45° with it. The substrate is placed in front of the target with its surface parallel to that of the target. Sufficient gap (3 cm) is kept between the target and the substrate. The substrate was heated by using a halogen lamp (1000W) to raises the substrate temperature to $300^\circ C$, K-type thermocouple was used to measure this temperature.

High purity (99.999%) MgO and ZnO powders supplied from Fluka company were first weighted at different concentrations and mixed with corresponding concentrations in a beaker filled with methanol by magnetic stirrer for 1 hour. After the liquid was dry out, the mixed powder was blended mechanically again, so that the mixture is uniformly distributed. The resultant powder was ground and pressed in hydraulic press with 5 ton pressure to form a target with 2.5 cm diameter and 0.4 cm thickness.

The $Mg_xZn_{1-x}O$ thin films were deposited on a sapphire (0001) substrate ($\alpha-Al_2O_3$ single crystal sapphire wafer (MTI Corporation)) heated at $300^\circ C$, $1.6 J/cm^2$ laser fluence, with an oxygen background pressure 2×10^{-1} mbar, and with different Mg content ($x=0, 0.1, 0.2, 0.3, 0.4, 0.6, 0.8, 1$). Prior to deposition, all polished sapphire substrates were etched in $H_2SO_4:H_3PO_4=3:1$ followed by ultrasonic cleaning in deionized water, and finally dried. The structure properties of prepared thin films were measured by using X-ray diffractometer (XRD 6000, shimadzu, Japan, $\lambda = 1.5406 \text{ \AA}$ from $Cu-K\alpha$). The surface morphology and especially the effect of the grains formation on the quality of the thin-film surface was measured by using atomic force microscopy (AFM) (SPM AA3000, Angstrom advanced Inc. USA).

A double-beam Spectrophotometer (SP-8001 UV-VIS, metertech Inc. version 1.08, Taiwan) was used to measure the transmittance and absorption of $Mg_xZn_{1-x}O$ thin films in the range (200-900) nm. The background correction is taken for each scan. The transmittance and reflectance data can be used to calculate absorption coefficients of the films at different wavelength, and used to determine the band gap energy E_g .

RESULTS AND DISCUSSION

x-ray diffraction measurements

The crystallinity of $Mg_xZn_{1-x}O$ films was investigated by measuring XRD patterns as shown in Figure (1) for $x=0, 0.2$ and 0.4 . Highly c -axis oriented ZnMgO (0002) reflections corresponding to the wurtzite-phase crystal structure (hexagonal structure) were observed for the films of $x=0$ (pure ZnO) and $x=0.2$, showing that these films grow epitaxially in a single crystalline phase on (0006) Al_2O_3 substrates without any rocksalt-phase structure. There was a systematic shift of ZnO (0002) peak towards higher diffraction angle with the increase in Mg contents. The increase in the Mg contents above to $x=0.4$ did not form complete solid solution. However, Mg segregates in the form of MgO, which is clearly visible by the presence of MgO (111) and (200) diffraction lines which indicates the co-existence of two phases (hexagonal and cubic structure).

Optical properties measurements

Figure (2) shows the optical transmittance spectra of the $Mg_xZn_{1-x}O$ films grown on a sapphire substrate at $300^\circ C$ substrate temperature, oxygen pressure 2×10^{-1} mbar with $1.6 J/cm^2$ laser fluence and different Mg-content, ($x=0.0 - 1$). Spectra display a clear continuous shift in the transmission edge.

The transmission spectrum for $x=0.4$ clearly showed two absorption edges which indicates the presence of secondary phase. This can be also correlated with XRD results, which show the presence of both cubic and hexagonal phases. These results are in agreement with other works^[6, 10].

The transmittance spectra of the films can be analyzed as follows:

1. The excitonic nature of the films is clearly apparent in the spectra. Because the exciton binding energy is almost the same as ZnO (≈ 60 meV)^[11] in the $Mg_xZn_{1-x}O$ thin films, the exciton peak remains present for all alloy compositions with increasing of Mg concentration.
2. Oscillations are observed in the transmittance spectra, which correspond to multi-reflexions at the film-air and film-substrate interfaces.
3. For all films, the average transmittance in the visible wavelength region ($\lambda = 400 - 800$ nm) is greater than 85%.
4. The transmittance of the $Mg_xZn_{1-x}O$ films increases as Mg content is increased.
5. The slopes of the absorption edge are softened and there is an obvious shift of the absorption edge towards lower wavelengths with increasing of Mg content. This may be attributed to the fact that new defects are introduced after substitute of Zn atoms in the ZnO lattice by Mg atoms due to the electronegativity and ionic radius difference between Zn and Mg^[12].

The optical band gap value can be extrapolated from the linear region by using the relation^[13]:

$$\alpha \cdot hv \approx A (hv - E_g)^{\frac{1}{2}} \quad \dots (2)$$

Where hv : incident photon energy, α : absorption coefficient, E_g : band gap energy, and A is constant.

Using this procedure, the optical energy band gap of Mg_xZn_{1-x}O thin films become wider as Mg content increases and can be precisely controlled between 3.4 and 5.9eV with increasing Mg-content from $x=0$ to $x=1$ as shown in Figure (3). The reason for observed blue shift in the band gap could be attributed to the higher band gap energy of MgO (≈ 7.7 eV).

The band gap at different spots on the spread extracted from optical measurements is shown in Figure (4). In the low Mg fraction region where the film remains wurtzite, the gap changes linearly from 3.4 to 4eV. In the mixed phase region for $x= 0.4$, $E_g= 4.3$ eV. In the cubic single-phase end of the phase diagram, the band gap increases nonlinearly from 5 to 5.9eV with increasing of Mg fraction.

The refractive index (n) can be found from transmittance spectrum of the film according to the following equation ^[12]:

$$n = \frac{1}{T} + \left[\frac{1}{T} - 1 \right]^{1/2} \quad \dots (3)$$

T : transmittance.

Figure (5) shows the variation in refractive index of Mg_xZn_{1-x}O films with wavelength at various Mg contents for $x= 0$ to $x=1$. The values of the refractive index for the films at $\lambda= 400$ nm vary in the range from 1.96 to 1.75 as Mg-content increased from 0 to 1. In other words, the refractive indices of the Mg_xZn_{1-x}O films are decreased as Mg-content increased as shown in Figure (6), which are less than those reported by Teng et al. ^[8].

Morphology measurements

Figures (7 and 8) show two and three dimensional of AFM images for the Mg_xZn_{1-x}O films deposited on sapphire substrate at fixed substrate temperature 300 °C, oxygen pressure 2×10^{-1} mbar, and laser fluence 1.6 J/cm² using different Mg contents ($x= 0, 0.2, 0.3, 0.8,$ and 1) with scanning area ($5 \times 5 \mu\text{m}$). It can be found that the root mean square (RMS) values of the surface roughness are 120.44nm, 72.1nm, 65.23nm, 38.74nm, and 30.22nm with $x= 0, 0.2, 0.3, 0.8,$ and 1, respectively. Figure (9) shows the variation of surface roughness with different Mg contents in the films.

It is found from the AFM results that the surface roughness of the films decreases with increasing the Mg content and this may indicate a grain growth inhibition effect by Mg atoms. This result is in agreement with the work of Jiet.al. ^[14, 15]. The values of RMS and mean grain size obtained from AFM images listed in Table (1).

CONCLUSIONS

In this work Mg_xZn_{1-x}O films were grown on sapphire substrates by using pulsed laser deposition. The optical properties of the Mg_xZn_{1-x}O films are found to be strongly dependent on the Mg content (x) in the films.

X-ray diffraction measurement shows that the present of hexagonal structure for $x=0.2$ and the co-existence of two phases (hexagonal and cubic structure) for $x=0.4$. The average transmission was 85% for all the films in the visible wavelength region ($\lambda =400\text{--}800$ nm), the transmittance of the Mg_xZn_{1-x}O films increases and the shift in the absorption edge towards lower wavelength (blue region) is clearly with increasing Mg

content. The band gap energy of ZnO become wider and changed from (3.4 – 5.9)eV as Mg content increases from 0 to 1, while the refractive index decreases from (1.96 – 1.75) as Mg-content increases from (0 to 1) at constant wavelength 400nm.

REFERENCES

- [1]. Kaushal, A. D. Pathak, R.K. Bedi, D. Kaur, "Structural, electrical and optical properties of transparent $Zn_{1-x}Mg_xO$ nanocomposite thin films", *Thin Solid Films* 518, p. 1394 (2009).
- [2]. Chen, N. B. H. Z. Wu, T. N. Xu, "Refractive indices of cubic-phase $Mg_xZn_{1-x}O$ thin-film alloys", *J. Appl. Phys.* 97, p. 023515 (2005).
- [3]. Sharma, A. K. J. Narayan, J. F. Muth, C. W. Teng, C. Jin, A. Kvit, R. M. Kolbas, O. W. Holland, "Optical and structural properties of epitaxial $Mg_xZn_{1-x}O$ alloys", *Appl. Phys. Lett.*, 75, 21, p. 3327 (1999).
- [4]. Makino, T. Y. Segawa, M. Kawasaki, A. Ohtomo, R. Shiroki, K. Tamura, T. Yasuda, H. Koinuma, "Band gap engineering based on $Mg_xZn_{1-x}O$ and $Cd_yZn_{1-y}O$ ternary alloy films", *Appl. Phys. Lett.*, 78, 9, p. 1237 (2001).
- [5]. Schleife, A. C. Rödl, J. Furthmüller, F. Bechstedt, "Electronic and optical properties of $Mg_xZn_{1-x}O$ and $Cd_xZn_{1-x}O$ from *ab initio* calculations", *New Journal of Physics*, 13, p. 085012 (2011).
- [6]. Choopun, S. R. D. Vispute, W. Yang, R. P. Sharma, T. Venkatesan, "Realization of band gap above 5.0 eV in metastable cubic-phase $Mg_xZn_{1-x}O$ alloy films", *Appl. Phys. Lett.*, 80, 9, p. 1529 (2002).
- [7]. Hang Huang, J. C. Pu Liu, "The influence of magnesium and hydrogen introduction in sputtered zinc oxide thin films", *Thin Solid Films* 498, p. 152 (2006).
- [8]. Ohtomo, A. M. Kawasaki, T. Koida, K. Masubuchi, H. Koinuma, Y. Sakurai, Y. Yoshida, T. Yasuda, Y. Segawa, " $Mg_xZn_{1-x}O$ as a II–VI widegap semiconductor alloy", *Appl. Phys. Lett.*, 72, 19, p. 2466 (1998).
- [9]. Teng, C. W. J. F. Muth, Ü. Özgür, M. J. Bergmann, H. O. Everitt, A. K. Sharma, C. Jin, J. Narayan, "Refractive indices and absorption coefficients of $Mg_xZn_{1-x}O$ alloys", *Appl. Phys. Lett.*, 76, 8, p. 979 (2000).
- [10]. Bhattacharya, P. Rasmi R. Das, Ram S. Katiyar, "Comparative study of Mg doped ZnO and multilayer ZnO/MgO thin films", *Thin Solid Films*, 447–448, p. 564 (2004).
- [11]. Gao, S. D. Li, Y. Li, X. Lv, J. Wang, Q. Yu, "Growth and characterization of ZnO nanorod arrays on boron-doped diamond films by low temperature hydrothermal reaction", *Journal of Alloys and Compounds* 539, p. 200 (2012).
- [12]. Kaur, D. A. Kaushal, "Effect of Mg content on structural, electrical and optical properties of $Zn_{1-x}Mg_xO$ nanocomposite thin films", *Solar Energy Materials & Solar Cells* 93, p. 193 (2009).
- [13]. Patel, T.H. "Influence of Deposition Time on Structural and Optical Properties of Chemically Deposited SnS Thin Films", *The Open Surface Science Journal*, 4, p. 6 (2012).
- [14]. Fang, L. W. Ji, C. M. Lin, T. H. T. T. Chu, H. Jiang, W. S. Shi, C. Z. Wu, T. L. Chang, T. H. Meen, J. Zhong, "Structural and optical properties of ZnO nanorods grown on $Mg_xZn_{1-x}O$ buffer layers", *Appl. Surf. Sci.*, 256, p. 2138 (2010).

[15]. Khandelwal, R. A. P. Singh, A. Kapoor, S. Grigorescu, P. Miglietta, N. E. Stankovad, " Effects of deposition temperature on the structural and morphological properties of thin ZnO films fabricated by pulsed laser deposition", Optics & Laser Technology,40, p. 247 (2008).

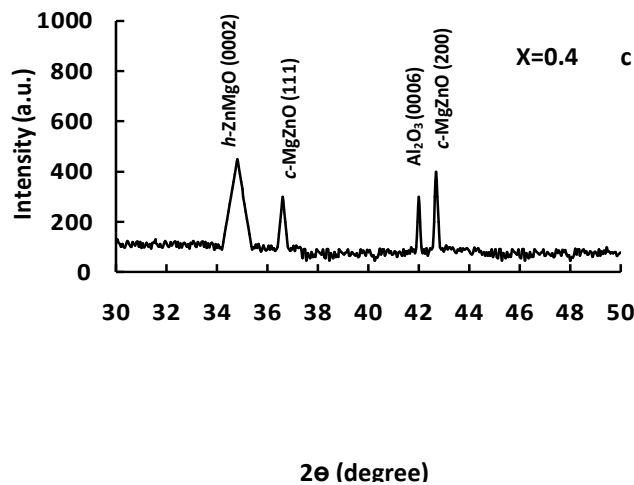
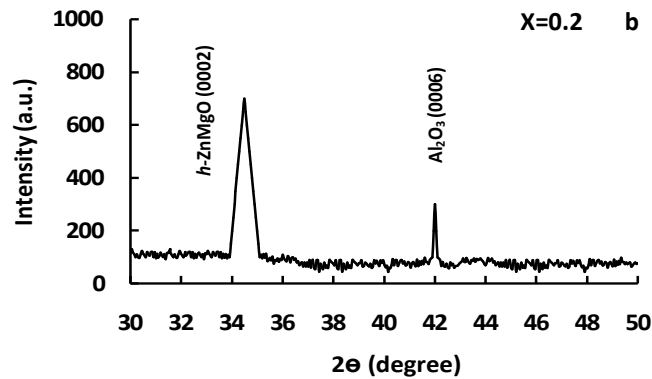
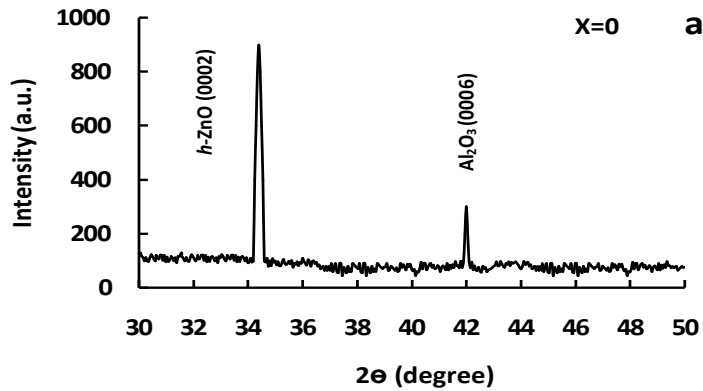


Figure (1) XRD spectra of $Mg_xZn_{1-x}O/Al_2O_3$ films deposited at Different Mg contents a) $x=0$, b) $x=0.2$ c) $x=0.4$.

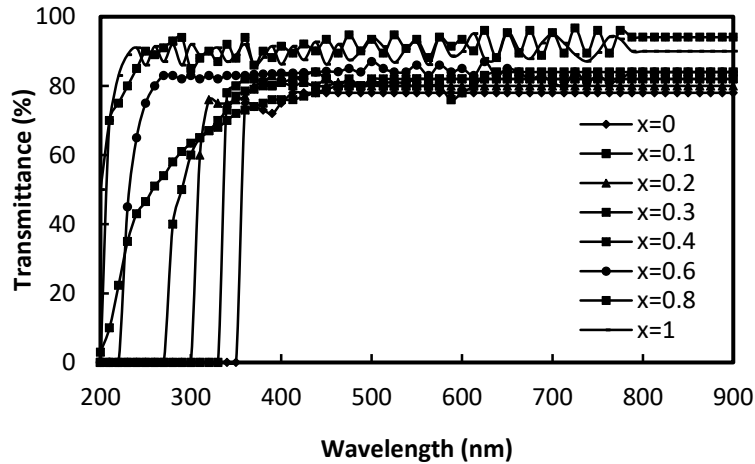
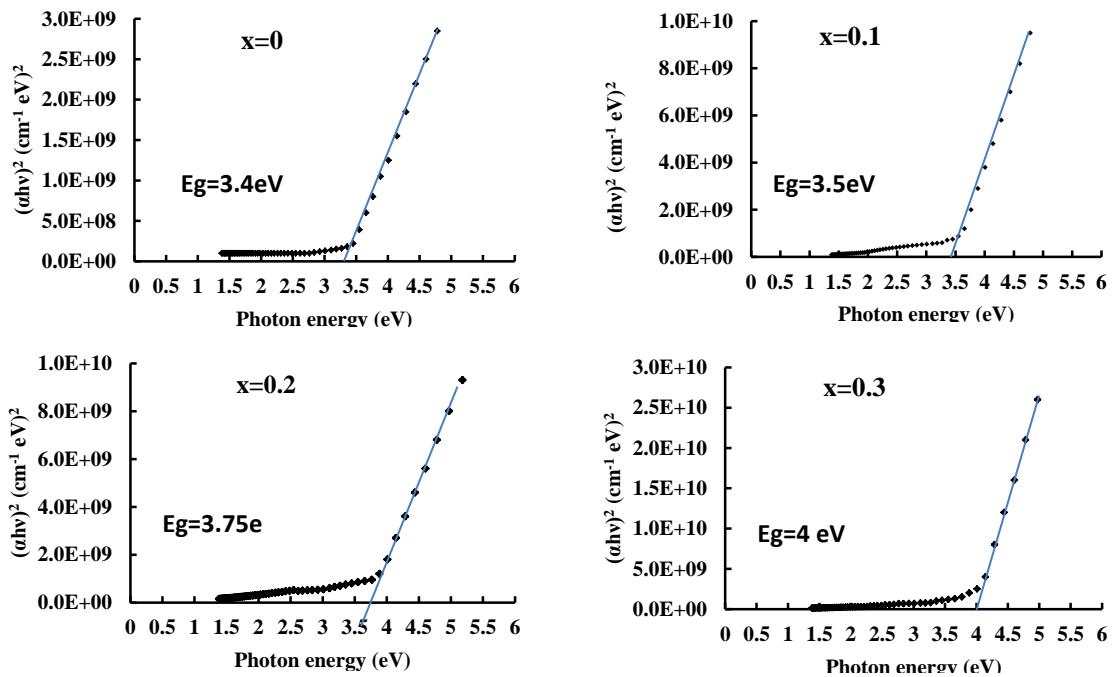


Figure (2) UV-VIS transmittance spectra of the $Mg_xZn_{1-x}O$ /Sapphire thin films with different Mg content.



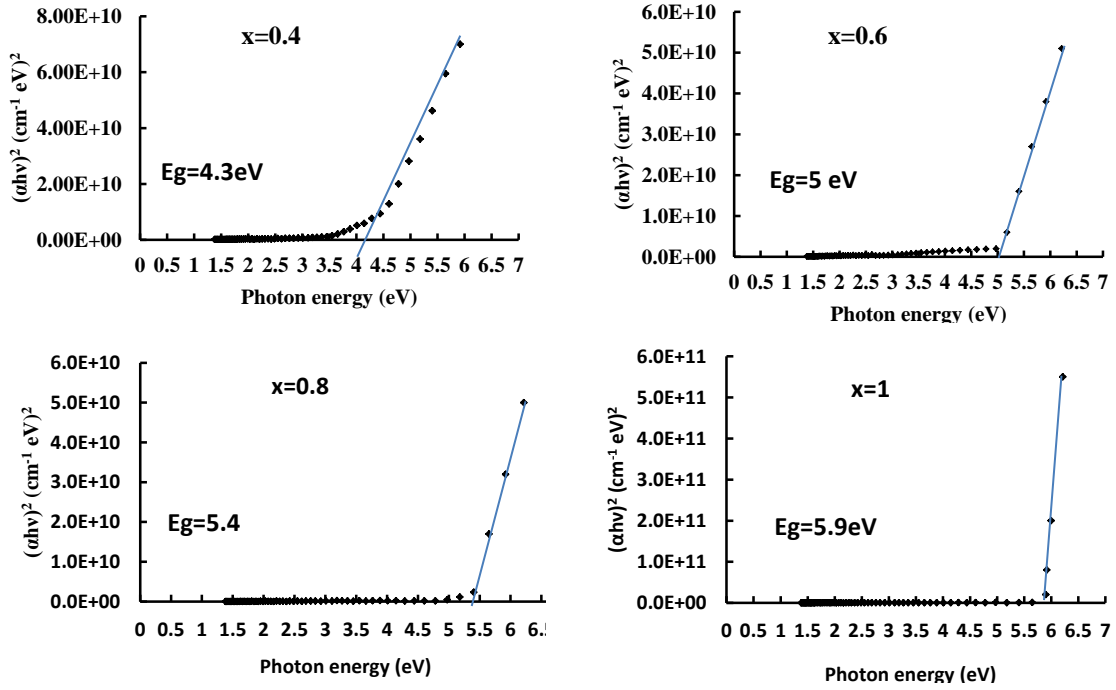


Figure (3) Variation of $(\alpha h\nu)^2$ Vs. $(h\nu)$ of $Mg_xZn_{1-x}O$ /Sapphire thin films with different Mg content.

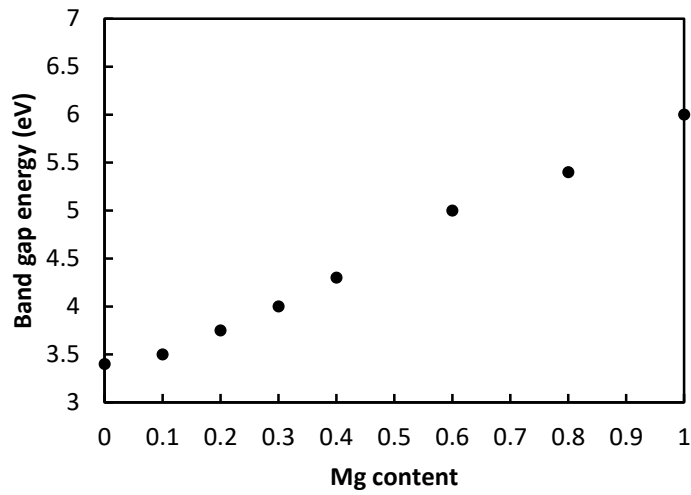


Figure (4) Band gap energy as a function of Mg content.

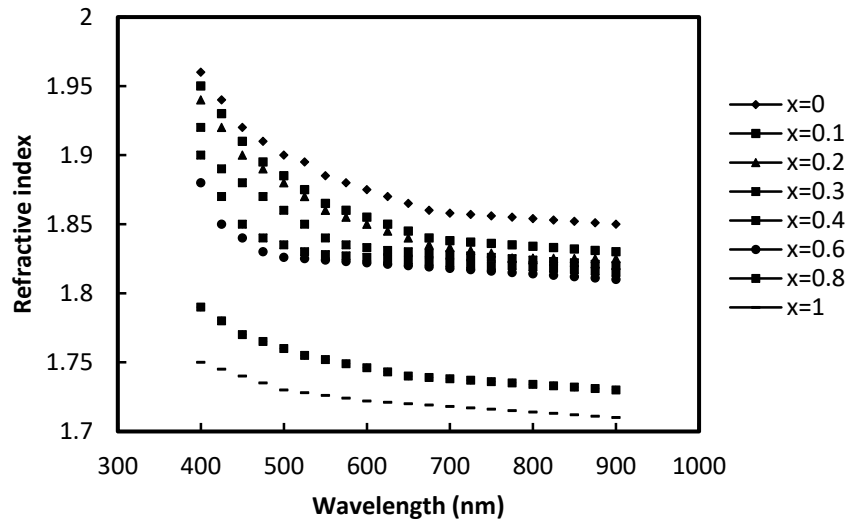


Figure (5) Refractive index as a function of wavelength for $Mg_xZn_{1-x}O$ films with different Mg content.

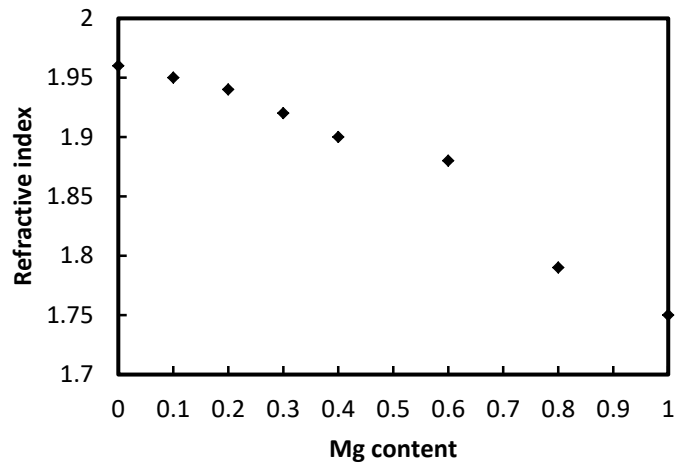


Figure (6) Refractive index as a function of Mg Content for $Mg_xZn_{1-x}O$ films at $\lambda=400nm$.

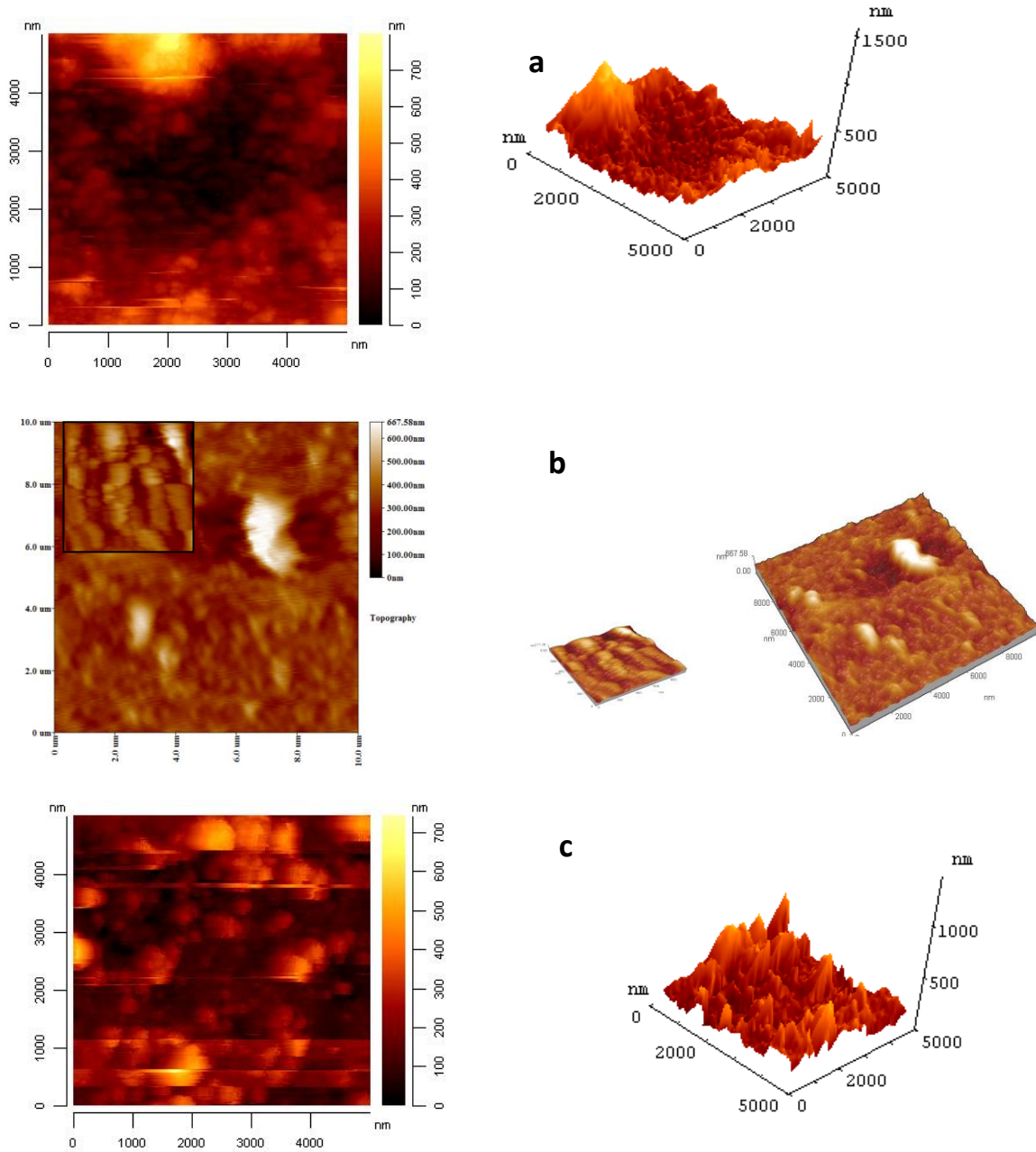


Figure (7) AFM images of the $Mg_xZn_{1-x}O$ /sapphire films with different

Mg contents a) $x=0$, b) $x=0.2$, c) $x=0.3$.

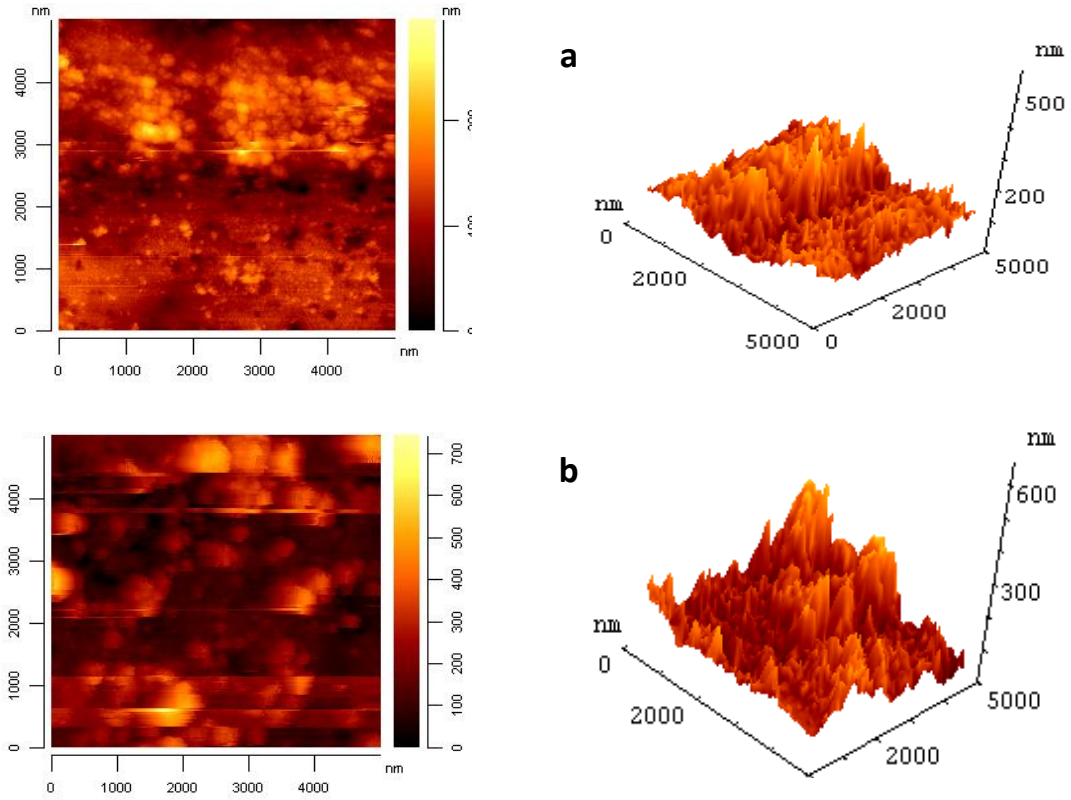


Figure (8) AFM images of the $Mg_xZn_{1-x}O$ /sapphire films with different Mg contents a) $x=0.8$, b) $x=1$.

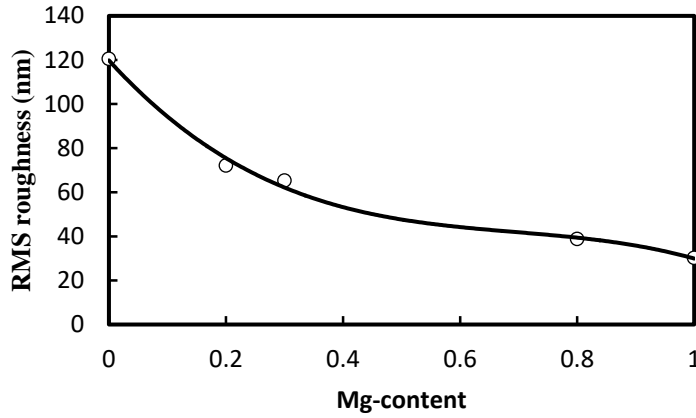


Figure (9) The variation of surface roughness with Mg- content in the $Mg_xZn_{1-x}O$ films deposited on sapphire substrate.

Table (1) AFM characteristics of the $Mg_xZn_{1-x}O$ /Sapphire films Deposited at different Mg content.

Mg- Content (x)	RMS Roughness (nm)	Mean Grain Size (nm)
0	120.44	52.4
0.2	72.1	42.7
0.3	65.23	40.1
0.8	38.74	37.5
1	30.22	33.8